

# The Ising model in a Bak-Tang-Wiesenfeld sandpile

Zbigniew Koza

*Institute of Theoretical Physics, University of Wrocław, pl. M. Borna 9, 50204 Wrocław, Poland*

Marcel Ausloos

*SUPRATECS, B5, Liège, Belgium*

(Dated: February 3, 2008)

We study the spin-1 Ising model with non-local constraints imposed by the Bak-Tang-Wiesenfeld sandpile model of self-organized criticality (SOC). The model is constructed as if the sandpile is being built on a (honeycomb) lattice with Ising interactions. In this way we combine two models that exhibit power-law decay of correlation functions characterized by different exponents. We discuss the model properties through an order parameter and the mean energy per node, as well as the temperature dependence of their fourth-order Binder cumulants. We find (i) a thermodynamic phase transition at a finite  $T_c$  between paramagnetic and antiferromagnetic phases, and (ii) that above  $T_c$  the correlation functions decay in a way typical of SOC. The usual thermodynamic criticality of the two-dimensional Ising model is not affected by SOC constraints (the specific heat critical exponent  $\alpha \approx 0$ ), nor are SOC-induced correlations affected by the interactions of the Ising model. Even though the constraints imposed by the SOC model induce long-range correlations, as if at standard (thermodynamic) criticality, these SOC-induced correlations have no impact on the thermodynamic functions.

PACS numbers: 05.65.+b; 45.70.Ht; 75.10.Hk;

## I. INTRODUCTION

The phenomenon of self-organized criticality (SOC) attracts a lot of interest in various branches of science (see [1, 2] for reviews). Its most intriguing feature resides in the “spontaneous” formation of scale-free spatio-temporal patterns with power-law correlations between various quantities. On the one hand, these correlations closely resemble those that appear at critical points in continuous phase transitions. On the other hand, while the critical state in phase transitions is temperature- or external-field-driven, a SOC state is thought to form without fine-tuning of any external parameters. The relation between the “classical” and “self-organized” criticality has been studied by many authors [2, 3, 4, 5] with a conclusion that the origin of the self-organized criticality is a continuous absorbing-state phase transition to which a SOC system is attracted.

Perhaps the best-known and most extensively studied model of thermodynamic criticality is the Ising model of ferromagnetism. Of similar importance for self-organized criticality is the Bak-Tang-Wiesenfeld (BTW) model [6] of a sandpile. Owing to its elegant mathematical structure and many rigorous results [7, 8, 9, 10], the BTW model has practically become a paradigm for self-organized criticality studies.

Specific SOC features of the BTW model, which will attract our attention, include the fact that in the BTW model correlation functions decay with the distance  $r$  as  $r^{-2d}$ , where  $d$  is the space dimensionality [11, 12], which resembles, but differs from the  $r^{-(d-2+\eta)}$  decay in standard critical phenomena. As the behavior of a correlation function is a key ingredient of criticality, we will use this property to build and analyze a model which, by con-

struction, is expected to exhibit long-range correlations induced by both classical and self-organized critical phenomena. In defining such a model we follow the idea of Ref. [13]: take a standard model of statistical physics and significantly reduce its phase space to that of a corresponding SOC model.

One of the main results of ref. [13], where a combination of the Potts and BTW models was investigated, is that in the limit of a vanishingly small temperature their hybrid system loses its ‘self-organized criticality’, i.e. the power-law correlations disappear. Thus it seems worthwhile to investigate a hybrid model, numerically, for a wide range of temperatures. In particular, we want to check if the self-organized criticality imposed by nonlocal constraints can be detected in the behavior of thermodynamic functions. However, as it was pointed out in Ref. [13], because of the non-local nature of the applied constraints, analysis of this type of models is a difficult problem, still at its infancy, so it is of interest to check whether standard concepts and theorems of statistical physics, like existence of the thermodynamic limit, ergodicity, fluctuation-dissipation theorem or the central limit theorem apply to such hybrid systems.

In our study we choose the two-dimensional spin-1 Ising model as the Hamiltonian system and the BTW sandpile model as the SOC component. The resulting model is an equilibrium model that takes (short-range) interactions from the Ising model and the (non-local) constraints from the BTW model. Note, however, that while the Ising model focuses on spin configuration at thermodynamical equilibrium, the BTW model attempts to describe a nonequilibrium, dynamical process where grains of sand are continually added to the lattice to form “avalanches” of different sizes and durations.

The construction of such a “hybrid” model employs the

fact that both component models are built on a lattice with special variables (“spins”  $s_j$  or “grain heights”  $h_j$ ) attached to each lattice node, and the values of these variables are limited to a few integers, e.g.  $s_j \in \{-1, 0, 1\}$  or  $h_j \in \{0, 1, 2\}$ . This property allows us to map the states of one model onto the states of the other one. To reduce to the minimum the number of possible mappings of the spins  $s_j$  of the Ising model to the sand heights  $h_j$  of the BTW sandpile, we choose a two-dimensional (2D) honeycomb lattice (coordination number  $z = 3$ ).

In a hybrid system like this the high-temperature limit is determined entirely by the constraints of the SOC component; consequently, the spin correlation function should decay with the distance  $r$  as  $r^{-4}$  [11, 12]. On the other hand, the ground state is expected to be controlled mainly by the Hamiltonian, and at sufficiently low temperatures interactions should force the system into an ordered phase. Consequently, one can expect a thermodynamic phase transition at some finite temperature  $T_c$ . For the standard 2D Ising model without an external field this transition is continuous and the spatial correlations decay as  $r^{-\eta}$  with  $\eta = 1/4$  [14]. Therefore, if introduction of the SOC constraints turns out to be too weak to change the nature of this transition, the hybrid model should exhibit a power-law decay of correlation functions both for  $T \rightarrow \infty$  and at  $T_c$ .

Although the Ising model has been modified in many, many ways, most of the modifications are of local character. These include building the model on fractal [15] or small-world [16] lattices as well as introduction of quenched [17, 18] or kinetic [19, 20] disorder. In our present approach the modification is nonlocal – one has to scan the whole lattice to decide whether a given configuration is allowed or not. This introduces several complications, but at the same time opens new directions of research. In our analysis we shall consider both the effects of introducing interactions and temperature to a SOC model and the changes introduced by a SOC-like constraints into a Hamiltonian system.

The paper is organized as follows. In section II we define the model. Then, in section III we discuss problems that appear in Monte Carlo simulations and we present some methods that we have applied to overcome them. The results are presented in section IV. They include a numerical analysis of the finite-size effects imposed by the SOC subsystem, an analytical study of the influence of the sandpile model on the number of phases in the Hamiltonian subsystem, and a numerical analysis of the impact of the SOC and Hamiltonian components on the critical properties of the system. It also contains results of several tests carried out to verify if the hybrid model with nonlocal constraints can be treated with standard methods of statistical physics. These include tests of whether fluctuations of the internal energy can be used to determine the specific heat and whether far from the critical point the central limit theorem can be applied to predict the distribution of the energy fluctuations. Finally, section V is devoted to conclusions.

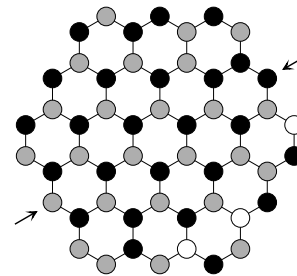


FIG. 1: An example of an allowed BTW configuration on a honeycomb lattice of linear size  $L = 3$ . Empty, shadowed, and filled circles represent the nodes with heights  $h_j = 0, 1, 2$  (or spins  $s_j = 0, -1, +1$ ), respectively. The arrows show an example of a pair of boundary nodes that interact via the Ising Hamiltonian (1).

## II. MODEL

We define the model on a two-dimensional honeycomb lattice of linear size  $L$ . An example of such a lattice with  $L = 3$  is shown in Fig. 1. The lattice has a shape of a big hexagon made of  $3L(L-1) + 1$  small hexagons and it has  $N = 6L^2$  nodes. Most of them are interior nodes connected to 3 nearest neighbors, but  $6L$  nodes lie on the edge of the lattice and have only 2 connections.

Each node  $j$  can be in one of three states, which can be interpreted either as a spin variable  $s_j \in \{-1, 0, 1\}$  or the number of sand grains  $h_j \in \{0, 1, 2\}$ . Of 6 mappings of heights  $h_j$  on spins  $s_j$ , we choose the one in which  $h_j = 0, 1, 2$  corresponds to  $s_j = 0, -1, +1$ , respectively (actually, due to the  $Z_2$  symmetry, the number of non-equivalent mappings reduces to 3).

The Hamiltonian of the model is simply that of the spin-1 Ising model,

$$H = -J \sum_{\langle i,j \rangle} s_i s_j \quad (1)$$

where  $J$  is a real parameter,  $s_j = 0, \pm 1$ , and the sum is to be taken over all pairs of nearest neighbors. To minimize finite-size effects, we have adopted periodic boundary conditions. To this end we assume that, as is illustrated in Fig. 1, each boundary node interacts, via (1), not only with its two direct lattice neighbors, but also with the node at the location symmetric about the lattice center. This choice ensures that the ground state in the antiferromagnetic case ( $J < 0$ ) is doubly degenerated and, together with the several consecutive excited states, obey the  $Z_2$  symmetry.

In the standard spin-1 Ising model the phase space is defined by all possible spin configurations. To each such configuration  $\eta$  one can assign a non-vanishing temperature-dependent probability  $\propto \exp[-H(\eta)/k_B T]$ , and their number is exactly  $3^N$ . However, the states of the BTW model, which is a dynamic, nonequilibrium model of a sand pile in a continual flux of sand grains, have completely different properties. It turns out that all

configurations can be divided into two categories: disallowed and allowed. The former can never be found in the steady state, while the latter can be found with the same probability [7, 8, 9]. Moreover, the number of allowed configurations is  $a^N$  with  $a < 3$  [8]; hence the number of allowed configurations is only a fraction of all configurations and this fraction tends to 0 as  $L \rightarrow \infty$ .

The main idea behind building a hybrid Hamiltonian-SOC model is to take a standard model of equilibrium statistical physics, e.g. the spin-1 Ising model, and significantly reduce its phase space to that of a corresponding SOC model, e.g. the BTW model. Solving a hybrid model is then equivalent to finding the partition function

$$Z = \sum_{\eta} \Theta(\eta) \exp[-H(\eta)/k_B T], \quad (2)$$

where the sum runs over all states  $\eta$  of the Hamiltonian component,  $\Theta$  is the characteristic function of a SOC state,

$$\begin{aligned} \Theta(\eta) &= 1, & \text{if } \eta \text{ is allowed} \\ \Theta(\eta) &= 0, & \text{if } \eta \text{ is disallowed} \end{aligned}$$

and  $k_B$  is the Boltzmann constant.

To complete the definition of the model, it remains to explain how to distinguish an allowed configuration from a disallowed one in the BTW model. A complete discussion of this problem is given by Dhar in [7, 8]; here we will give only a brief summary of his results: (i) a configuration with all  $h_j = 2$  is allowed. (ii) If we take an allowed configuration  $\{h_j\}$  and increase the value of  $h_j$  at some  $j$  by one, this  $h_j$  may exceed the maximum value 2; however, if we then relax such an “unstable” state (in the way defined below), we will always arrive at an allowed configuration. (iii) All allowed configurations can be reached by iteratively applying step (ii) to any allowed configuration. Relaxation of unstable states is carried out as follows: for any site  $j$  at which  $h_j > 2$ , replace  $h_j$  with  $h_j - 3$  and for every neighbor  $k$  of  $j$  increase  $h_k$  by 1. Relaxation of any state can be carried out in arbitrary order, consists of a finite number of steps that form the so called avalanches and the resulting stable state is unique [7, 8]. An example of an allowed configuration is shown in Fig. 1. Note that while we use periodic boundary conditions for the Hamiltonian part of the model, we employ open BC for the relaxation process so that excessive “sand grains” can leave the system.

### III. NUMERICAL IMPLEMENTATION

Most sandpile models studied so far are characterized by irreversible dynamics, where one only *adds* grains which later leave the system through open boundaries. Thus, if by adding a grain to a stable state  $X$  and relaxing it one arrives at another stable state  $Y$ , there is usually no way to return from  $Y$  to  $X$  in just one step. As this

violates the detailed-balance condition and hence drives the system out of equilibrium, in our simulations we also use the method of Ref. [21] to construct the reversed process that transforms  $Y$  back to  $X$ . This method is based on removing a grain from an (arbitrary) node and then fully relaxing the resulting state.

Following the standard Metropolis algorithm [22, 23], in each time step we construct a trial state by picking at random a lattice node  $j$  and adding or removing a grain at it. If this renders the configuration unstable, an avalanche is generated and the system is fully relaxed to a stable state. We then calculate the energy of the trial state,  $E'$ , compare it with the energy of the original state,  $E$ , and accept the trial state with probability  $\min(1, \exp[-(E' - E)/k_B T])$ . This, however, may lead to problems with ergodicity. Since the phase space of our model is limited to recurrent states of a Markov process defined by the BTW model, there is no doubt that at least in theory the system is ergodic. However, some transition probabilities can be extremely small. This problem can be particularly serious for transitions related to large avalanches, as in their case the factor  $\exp[-(E' - E)/k_B T]$  can quickly tend to 0 as  $L \rightarrow \infty$ .

Calculation of a trial state in our model is extremely time-consuming, for it requires to perform full relaxation of an excited state, and the average number of individual topplings in an avalanche is proportional to the number of lattice nodes  $N$  [7]. For this reason we were able to perform simulations only for rather small lattices with  $N \leq 9600$  (for a pure Ising or BTW models this number could be easily increased by a factor 1000). Due to the non-local nature of sandpile dynamics employed to generate trial states, there seems to be no way to apply here any of the many techniques for speeding up Monte-Carlo simulations [23]. The only ‘trick’ we used was to store, for a given configuration, energies of any rejected Monte-Carlo trial steps to avoid multiple relaxations of the same state. For low temperatures this can speed up calculations by a factor of 100.

## IV. RESULTS

### A. Finite-size effects induced by the BTW component

Two essentially different types of finite size effects can be expected to appear in the model. The first kind, typical of critical points, results from the fact that at criticality the diverging correlation lengths exceed the system size. The second kind is inherent to SOC models with open boundaries, as the mean concentration of particles near the open boundaries tends to be smaller than that in the bulk. For a two-dimensional lattice of linear size  $L$  this phenomenon brings about a finite-size correction of order  $O(1/L)$  [24]. This finite-size effect has a noticeable impact on the thermodynamics of the hybrid model *at all temperatures*. Its magnitude can be appreciated by

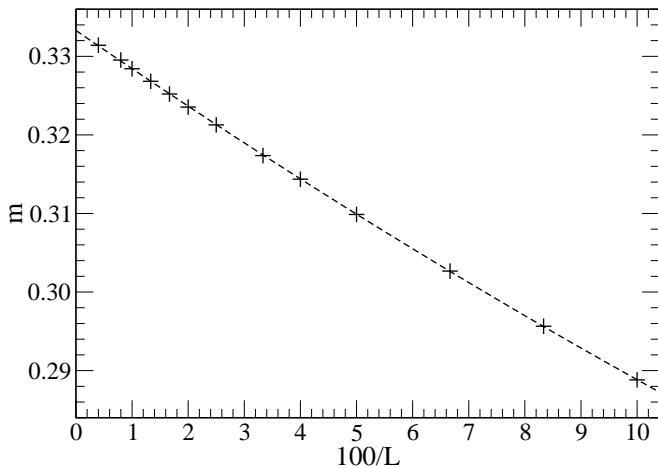


FIG. 2: Order parameter  $m$  as a function of  $L^{-1}$  for lattice sizes  $L = 10, \dots, 250$ . The error bars are less than the line width. The dashed line represents a quadratic fit and the extrapolated value for  $L \rightarrow \infty$  is 0.33330(4).

studying the limit of the temperature going to infinity, since in this case our model is governed entirely by its SOC component.

Although the finite-size effects in the BTW model were investigated in several papers [24, 25], none of them referred to the honeycomb lattice. Figure 2 depicts  $m = \langle s_j \rangle$ , i.e. the order parameter in the standard Ising model (magnetization per node), for several values of the system size  $L$ . As expected, the dependence of this parameter on  $L$  is quite strong. Upon approximating  $m(L)$  as a quadratic in  $1/L$  and extrapolating it to the limit of  $L \rightarrow \infty$ , we obtained  $m_\infty \approx 0.33330(4)$ , which suggests that  $m_\infty = 1/3$ . Note that in our model  $m > 0$  even at infinite temperature and in absence of an external magnetic field. This reflects a property of the BTW sandpile model that nodes with 2 grains (corresponding to  $h_j = 2$ , or  $s_j = +1$ ) are more probable than those with 1 grain ( $h_j = 1$ , or  $s_j = -1$ ).

Similarly good quadratic fits were found for the mean concentrations  $c_L^{(0)}$ ,  $c_L^{(1)}$ , and  $c_L^{(2)}$  of nodes with  $h_j = 0, 1$  and  $2$ , respectively. In the limit of  $L \rightarrow \infty$  we obtained  $c_\infty^{(0)} \approx 0.08334(5)$ ,  $c_\infty^{(1)} \approx 0.29166(2)$ , and  $c_\infty^{(2)} \approx 0.62500(3)$ . This suggests that  $c_\infty^{(0)} = 2/24$ ,  $c_\infty^{(1)} = 7/24$ , and  $c_\infty^{(2)} = 15/24$ . Note that the exact values of  $c_\infty^{(k)}$  are known for square [26] and Bethe [24] lattices, and numerical results are available for hypercubic lattices of dimension 2 to 5 [24].

### B. Effect of SOC constraints on possible phases of the Hamiltonian system

As we have just seen, the high-temperature properties of our model are very unusual: while in standard Hamiltonian systems at high temperatures the magnetization disappears (the system is in a disordered, paramagnetic

phase), our hybrid system exhibits a nonzero, positive  $m$  as  $T \rightarrow \infty$ . Moreover, we will show that  $m \geq 0$  in the limit  $L \rightarrow \infty$  (of an infinite system), at any temperature and for any values of the control parameter  $J$ .

Let  $N_k$  denote the total number of lattice nodes with  $k$  grains,  $k = 0, 1, 2$ . On the one hand their sum is the total number of lattice nodes,

$$N_2 + N_1 + N_0 = 6L^2. \quad (3)$$

On the other hand, in any allowed configuration these numbers satisfy

$$2N_2 + N_1 \geq B_L, \quad (4)$$

where  $B_L$  is the number of bonds on a lattice of size  $L$ . This relation can be justified using the original version of the burning algorithm [7, 8], which guarantees that the  $B_L$  bonds can be mapped onto the  $N$  nodes in such a way that a node with  $k$  grains is an image of at least  $k$  bonds.

Equation (3) implies  $c_L^{(2)} + c_L^{(1)} \leq 1$  and, since in our case  $B_L = 9L^2 - 3L$ , equation (4) leads to  $2c_L^{(2)} + c_L^{(1)} \geq 3/2 - 1/2L$ . Hence

$$m_L = c_L^{(2)} - c_L^{(1)} = 2(2c_L^{(2)} + c_L^{(1)}) - 3(c_L^{(2)} + c_L^{(1)}) \geq -1/L. \quad (5)$$

As the right-hand-side of this relation tends to 0 as  $L \rightarrow \infty$ , we conclude that there can be no phase with a negative value of  $m$ . This is not a trivial statement, as for suitably chosen values of  $J$  and  $T$ ,  $m$  can take on any value in the range  $[0, 1]$ , and for finite lattices there even exist allowed configurations with  $m < 0$ . An example of a system with  $m < 0$  is a lattice with  $L = 1$  in which one node has a high  $h_j = 2$  (corresponding to the spin  $s_j = +1$ ) and the remaining 5 nodes have  $h_j = 1$  (i.e.  $s_j = -1$ ). Since (5) applies to systems at an arbitrary temperature, it implies that no paramagnetic-ferromagnetic phase transition at finite  $T$  is possible in the hybrid model, so that the parameter  $m$  cannot be regarded as a usual magnetization.

Similar arguments lead to  $c_L^{(0)} \leq 1/4 + 1/4L$ , which implies that no quadrupolar phase is possible in the model (in a quadrupolar phase half of the nodes have spins  $s_j = 0$ , i.e.  $c_L^{(0)} \geq 1/2$ ). Consequently, only two phases can exist: a high- $T$  paramagnetic ( $P$ ) and a low- $T$  antiferromagnetic ( $A$ ) phase. Note that this reduction of the number of possible phases is a consequence of the constraints imposed on the Ising model by the sandpile dynamics, and has nothing to do with the “criticality” of the latter.

These conclusions are in accord with symmetry considerations. Because of the constraints imposed by the underlying SOC model, the hybrid model has a single, unique “ferromagnetic” ground state, and hence the low- $T$  system with ferromagnetic coupling ( $J > 0$ ) is not invariant under the  $Z_2$  symmetry of the standard Ising model; consequently, no ferromagnetic-like phase transition is expected in the system. On the other hand,

the SOC constraints do not affect the antiferromagnetic ( $J < 0$ ) ground state nor none of its “neighboring” (i.e. slightly excited) states. Thus, the hybrid model with antiferromagnetic coupling at low  $T$  obeys the antiferromagnetic  $Z_2$  symmetry, which opens a possibility of the antiferromagnetic phase transition.

### C. Transition between paramagnetic and antiferromagnetic phases

Since we expect the antiferromagnetic phase to appear only for  $J < 0$ , we decided to look for a temperature-driven transition between the  $P$  and  $A$  phases only for  $J < 0$ . For the sake of simplicity, we measure energy in units of  $|J|$  and set the Boltzmann constant  $k_B = 1$ . To investigate a phase transition, we formally divide the lattice into two sublattices (such that no adjacent nodes belong to the same sublattice) and we define a parameter  $a$  as half of the difference between magnetizations on each sublattice. In the ground state our system has a perfect antiferromagnetic order, with one sublattice completely filled with spins  $s = +1$ , and the other one with  $s = -1$ . Hence the mean energy per node  $u = -1.5$ , magnetization  $m = 0$  and the order parameter  $a = \pm 1$ . We expect that  $|a| > 0$  in the  $A$  phase, and  $a = 0$  in the high- $T$  phase.

We start each simulation from the ground state in phase  $A_+$  with  $a = 1$ , and then slowly warm the system up. After equilibrating, at each temperature we use an algorithm of [24] to generate  $10^8$  configurations. The results are averaged over 10 independent runs.

#### 1. Internal energy and specific heat

In Fig. 3 we present the temperature dependence of the internal energy per lattice node,  $u$ , calculated for a system of linear size  $L = 40$ . As can be seen, the curve has a quite large slope at  $T \approx 1.5$ . This suggests that the specific heat

$$C = du/dT. \quad (6)$$

may diverge near  $T = 1.5$ , which is the first hint for a phase transition. A blow-up of this region is presented in the inset, together with results for smaller lattices ( $L = 10$  and  $20$ ). It shows that the curves obtained for different lattice sizes cross each other at  $T_c \approx 1.475$  and suggests that near this temperature  $du/dT$  (i.e. the specific heat) significantly depends on the system size. Note that this value is different from the critical temperature of the standard spin-1 Ising model on a honeycomb lattice,  $T_c^{\text{Ising}} \approx 1.2$  [27, 28].

The temperature dependence of the specific heat, calculated for three different lattice sizes from energy fluctuations,

$$C = \frac{N}{T^2} \left( \langle u^2 \rangle - \langle u \rangle^2 \right), \quad (7)$$

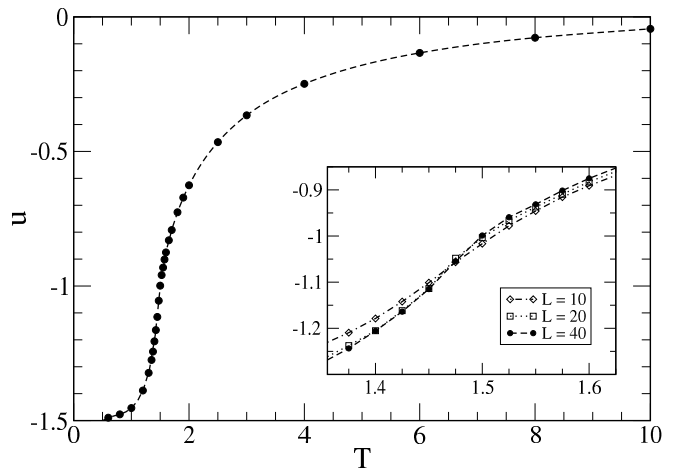


FIG. 3: Energy per lattice node,  $u$ , as a function of temperature for  $J < 0$  and lattice size  $L = 40$ . The inset presents the results for  $L = 40$  ( $\bullet$ ),  $L = 20$  ( $\square$ ), and  $L = 10$  ( $\diamond$ ) in the vicinity of  $T \approx 1.475$ .

is depicted in Fig. 4. As can be seen,  $C$  develops a maximum near  $T_c \approx 1.475$ , and this maximum grows with lattice size  $L$ . This  $L$ -dependence of  $C$  on the system size is far more significant near  $T_c$  than far from it and thus should be attributed to the classical phase transition rather than to the effects induced by the SOC constraints. The finite-size scaling theory predicts that if there is a second-order transition at  $T_c$ ,  $C(T_c)$  should grow as  $L^{\alpha/\nu}$ , with  $\alpha, \nu$  being the usual scaling exponents. The dependence of  $C$  at  $T = 1.475$  on  $L$  is shown in Figure 5 as a log-log plot. It suggests that the slope tends to 0, which implies  $\alpha = 0$ . This, in turn, suggests that the hybrid system could belong to the same universality class as the standard Ising model, for which  $\alpha = 0$ ,  $\nu = 1$ , and the specific heat diverges logarithmically. To verify this possibility, in Fig. 5 we also plotted a line which represents the best-fit of the data to the ansatz  $C(L) \approx a + b \ln(L)$ . The fit turns out to be rather convincing.

Notice the inset in Fig. (4). It depicts  $C(T)$  on a log-log plot. It can be observed that for large temperatures  $T$  the specific heat decays as  $T^{-2}$ , as it should do for usual Hamiltonian lattice spin models.

A well-established numerical method for analysis of critical points consists in studying the temperature dependence of the fourth cumulant of  $u$ ,

$$V_L = 1 - \frac{\langle u^4 \rangle}{3 \langle u^2 \rangle^2}. \quad (8)$$

This quantity is supposed to have a local minimum at  $T_c$ , both for continuous and discontinuous phase transitions [23, 29]. For first-order transitions the depth of this minimum,  $2/3 - V_L^{\min}$ , carries information about the latent heat. The dependence of  $V_L$  on temperature in our model is presented in Fig. 6. The curves develop a clear minimum near  $T = 1.475$ . Since its depth decreases with  $L$ , it suggests that there is no latent heat and the

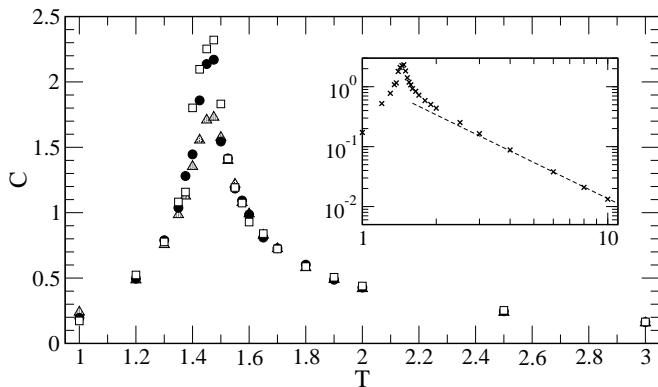


FIG. 4: Temperature dependence of specific heat  $C$ , Eq. (7), for  $L = 10$  ( $\blacktriangle$ ),  $20$  ( $\bullet$ ) and  $40$  ( $\square$ ). The inset presents a log-log plot of the same quantity (for  $L = 40$ ), with the dashed line showing an approximation of the form  $C(T) \propto 1/T^2$ .

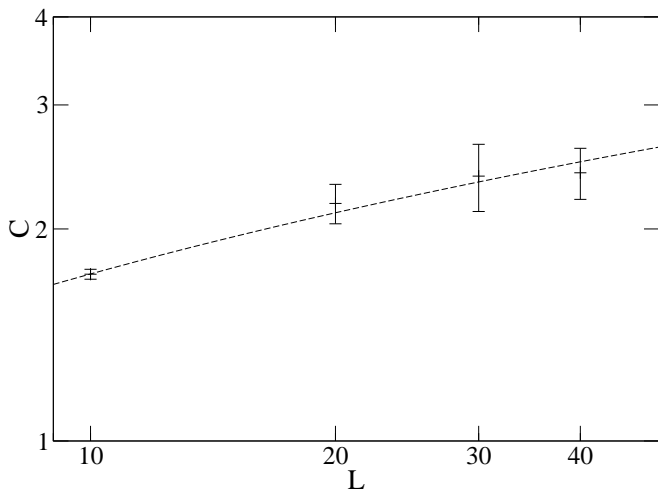


FIG. 5: Finite-size scaling of the specific heat  $C$  at  $T = 1.475$  (log-log plot). The dashed line is the best fit to the formula  $C(L) = a + b \ln(L)$ .

transition is of the second order.

At this point we apply two tests on  $u$  to see if our system has some basic properties of standard models of statistical physics. First, we verify whether the thermodynamic and microscopic definitions of specific heat, Eqs. (6) and (7), are equivalent. The result of this test is shown in Fig. 7, which presents  $C$  calculated with the two methods. The consistency of the results is very good. Second, we check if the distribution of energy (far from  $T_c$ ) is normal. An example of a result of this test is presented in the inset of Fig. 7, which shows a histogram of  $u$  as well as the best-fit Gaussian approximation. In this case the empirical and theoretical distributions are very close to each other.

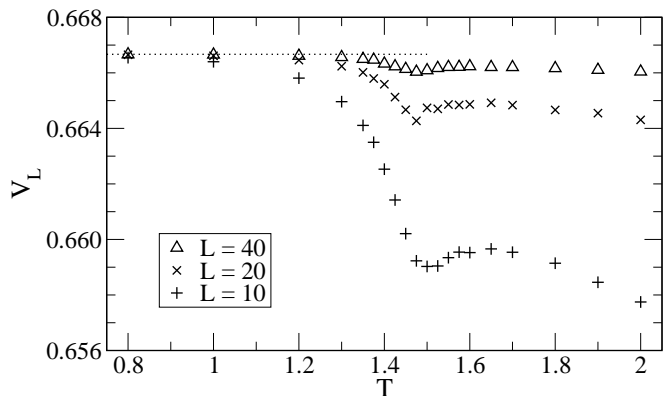


FIG. 6: Temperature dependence of the energy cumulant  $V_L$  for  $L = 10, 20$ , and  $40$ . The dotted line shows the theoretical value of  $V_L = 2/3$  as  $T \rightarrow 0$

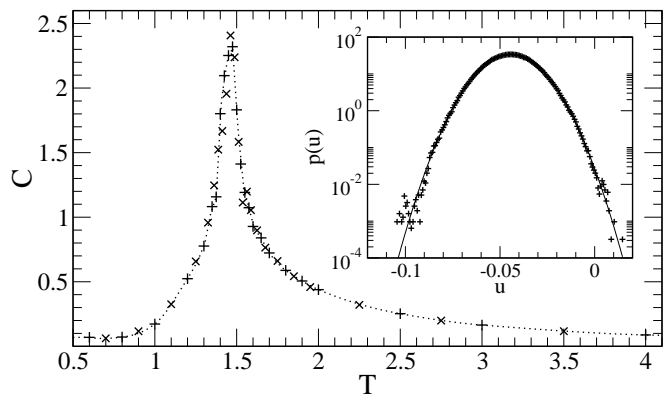


FIG. 7: Specific heat per node,  $C$ , for  $L = 40$ , calculated from energy fluctuations ( $+$  and dotted line) and the derivative  $du/dT$  ( $\times$ ). The inset depicts the histogram of internal energy for  $T = 10$  and  $L = 40$ . The solid line is the best-fit normal distribution.

## 2. The order parameter and Binder's cumulant

The temperature dependence of the antiferromagnetic order parameter  $|a|$  is depicted in Fig. 8. It shows that the graphs of  $|a(T)|$  for various system sizes  $L$  cross near  $T = 1.475$  (probably at different temperatures). In the same region the slope of  $|a(T)|$  gets steeper with increasing  $L$ , while for higher temperatures  $|a|$  quickly tends to 0 as  $L \rightarrow \infty$ . All these properties are typical hallmarks of a classical phase transition. However, large error bars (not shown) prevented us from doing any reliable quantitative estimates of the critical exponents or  $T_c$  based on these data.

We have also performed a study of Binder's cumulant, which is the fourth cumulant of the order parameter [23],

$$U_L = 1 - \frac{\langle a^4 \rangle}{3 \langle a^2 \rangle^2}. \quad (9)$$

This quantity is particularly useful in finding a critical

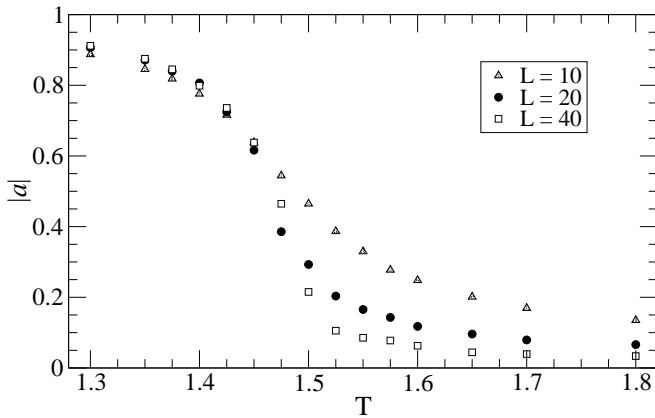


FIG. 8: The antiferromagnetic order parameter  $|a|$  as a function of temperature  $T$  for  $L = 10, 20$  and  $40$ .

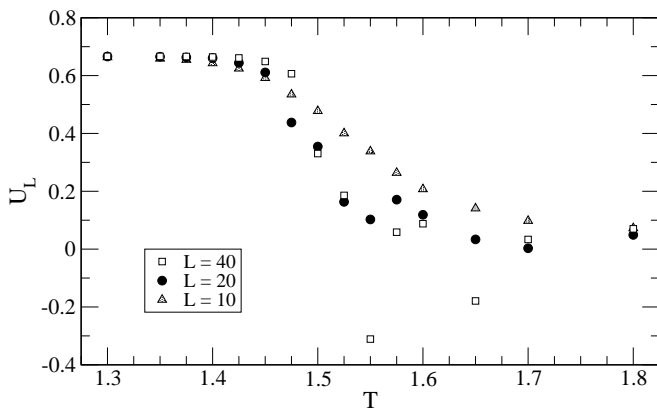


FIG. 9: Binder cumulant  $U_L$  as a function of temperature  $T$  for  $L = 10, 20$ , and  $40$ .

temperature,  $T_c$ , which can be extrapolated from the abscissas of intersection points of  $U_L(T)$  for several  $L$ , as these abscissas are typically only very weakly dependent on  $L$ . This method is supposed to give precise results irrespective of the order of the phase transition [23]. The plot of  $U_L(T)$  for our model is shown in Fig. 9. As can be seen, Binder's cumulants seem to cross each other, though the cutting point coordinates are loosely dependent on  $L$ . Moreover, the error bars (not shown), especially for larger temperatures, are very high.

To identify the source of these problems, we investigate histograms of the order parameter  $a$  at various temperatures. This is motivated by the fact that the theory behind Binder cumulant  $U_L$  is based on an assumption that these histograms can be approximated by a normal distribution in a disordered phase, and by a superposition of two normal distributions in an ordered phase. Four typical histograms are presented in Fig. 10. The first one shows that, for temperature  $T = 1.2 \ll T_c$ , the histograms are smooth functions of  $a$  that can be approximated by a Gaussian only for the largest system size ( $L = 40$ ); for small  $L$  they develop a slowly decaying tail on the left. The second panel shows the situation for

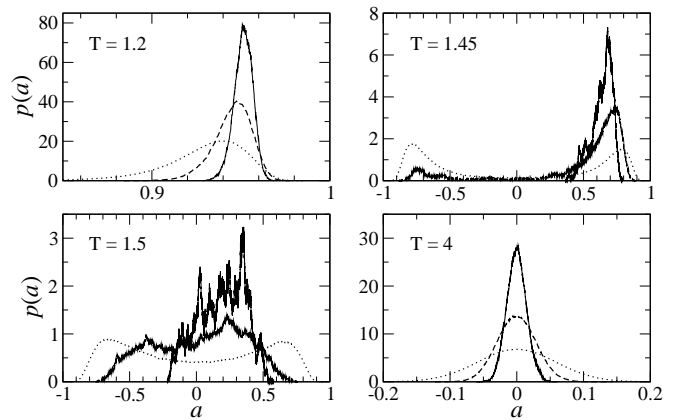


FIG. 10: The histograms of the antiferromagnetic order parameter  $a$  for  $T = 1.2, 1.45, 1.5, 4$  and three lattice sizes  $L = 10$  (dotted line),  $20$  (dashed line) and  $40$  (solid line, narrowest distribution).

$T = 1.45$ , which is just below  $T_c$ . For  $L = 10$  the system can freely switch between states with positive and negative  $a$ , but such a switch is impossible for  $L = 40$ . In the intermediate case of  $L = 20$ , the system can switch to  $a < 0$ , but the histogram is very asymmetric, which indicates that the actual relaxation time must be *much* larger than the simulation time. As illustrated in the third panel, at a little higher temperature  $T = 1.5$  the system can already freely switch between  $a > 0$  and  $a < 0$  for all investigated system sizes. However, the histogram for  $L = 40$  turns out asymmetric about  $a = 0$  and very erratic, which again indicates that the relaxation time is far larger than that available in computer simulations. Finally, the last panel shows that at a high temperature,  $T = 4$ , histograms are again smooth functions of  $a$ , and each can be approximated by a normal distribution. Therefore, for temperatures  $T \approx 1.475$  and large system sizes  $L$ , the actual relaxation time is much larger than the simulation time. Large relative errors of the data presented in Fig. 9 can thus be explained by the phenomenon of slow relaxation, which seems to be a generic property of sandpile models [30], and which should be particularly important at temperatures close to  $T_c$ .

#### D. Influence of the Ising interactions on criticality of the BTW subsystem

Recall that a signature of criticality is the power-law decay for the probability  $P_{kl}(r)$  that two nodes at a distance  $r$  apart have heights  $k$  and  $l$  ( $0 \leq k, l \leq 3$ ). It was proved [11] that in the bulk of a two-dimensional sandpile one has

$$P_{00}(r) = P_0^2 + cr^{-4} + \dots, \quad (10)$$

where  $P_0$  and  $c$  are some constants that depend on the lattice and boundary conditions [11]. This relation can be used as a test of the extent to which the self-organized

criticality is affected by temperature and interactions. The idea is simple: if for  $T > T_c$  the system is dominated by interactions,  $P_{00}(r)$  should decay in a way typical of high-temperature Hamiltonian systems, i.e. exponentially; if the system is dominated by SOC constraints,  $P_{00}(r)$  should decay in accordance with (10).

The results for a rather high temperature  $T = 10$ , where the Ising interactions should not play a significant role, are depicted in Fig. 11. The log-log plot in the inset confirms validity of Eq. (10). Similar results were also obtained for all temperatures  $T \gtrsim 2.5$ , whereas for  $T < 2.5$  an exponential fit was also possible. We explain this as follows. Generally one can expect that for temperatures  $T > T_c$  the decay rate of  $P_{00}(r)$  will have both power-law (SOC) and exponential (thermodynamic) contributions, the former proportional to  $1/r^4$  and the latter proportional to  $\exp(-r/\lambda)$ , where  $\lambda$  is the correlation length. For  $r$  large enough, the power-law should dominate, but for smaller distances, like those available in computer simulations,  $P_{00}(r)$  may be dominated by the exponential term, especially for temperatures closer to (but larger than)  $T_c$ , as in this case the thermodynamic correlation length gets large and the exponential term can exceed the rapidly decaying algebraic term  $1/r^4$ . Another reason why we did not confirm (10) for  $T < 2.5$  is that as the system gets cooler, the Ising interactions become more pronounced. As one of their effect is to reduce the number of sites with  $h_j = 0$ , the statistics for exploring  $P_{00}(r)$  becomes too poor for reliable data analysis.

Validity of equation (10) for  $T > T_c$  can be also justified by the following physical argument. Suppose that the role of interactions, above  $T_c$ , is restricted to flipping some spins from  $S_j = 0$  to  $S_j = \pm 1$ , with a probability  $p$ , in an *uncorrelated* manner. This reduces  $P_{00}(r)$  by a factor  $(1 - p)^2$ . Consequently,  $P_{00}(r)$  should satisfy (10) also for finite temperatures, with the ratio  $P_0^2/c$  independent of  $T$ . And indeed, our estimates of this ratio for  $T = 2.5, 3, 4, 6, 8$ , and  $10$  yield a constant value  $0.34 \pm 0.01$ .

We conclude that the system preserves the SOC-induced correlations at all temperatures  $T > T_c$ . Note, however, that this has absolutely no impact on the thermodynamic properties of the system.

## V. CONCLUSIONS AND OUTLOOK

We found that the spin-1 Ising model with nonlocal constraints imposed by the Bak-Tang-Wiesenfeld sandpile model, which is expected to exhibit some features of both thermodynamic and self-organized criticality, behaves just like a standard model of statistical physics, with all hallmarks of a continuous phase transition. Our analysis shows that the power-law correlations induced by the ‘self-organized criticality’ of the sandpile model have no impact on the order of the phase transition in the Hamiltonian subsystem. In particular, we found that the critical exponent  $\alpha \approx 0$ , which suggests that the

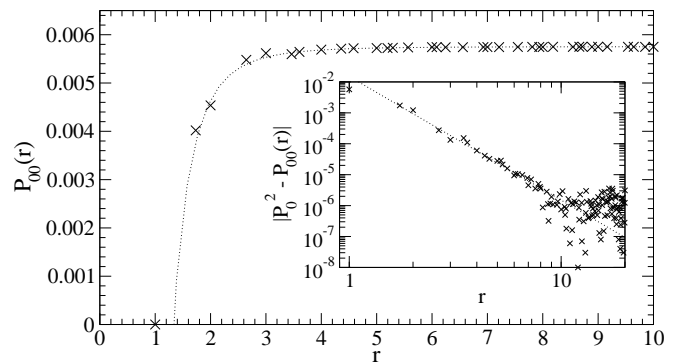


FIG. 11: Probability  $P_{00}(r)$  of finding two empty lattice nodes  $r$  units apart for  $L = 40$  and  $T = 10$ . The dotted line is a fit calculated from (10). The inset presents the log-log plot of  $|(P_0)^2 - P_{00}(r)|$ . The error bars are of order  $10^{-6}$  (not shown).

hybrid model belongs to the same universality class as the standard Ising model. Similarly, Hamiltonian interactions of the Ising model cannot destroy ‘criticality’ (i.e. power-law correlations) of the BTW sandpile model above the thermodynamic  $T_c$ . However, unlike thermodynamic criticality, long-range correlations induced by the self-organized criticality do not show up in thermodynamic functions (for example, they do not affect temperature dependence of the specific heat). Clearly, the long-range order induced by Hamiltonian interactions has different impact on the thermodynamics than that induced by using the SOC model to reduce the phase space of the system.

Even though the spin and sandpile models we chose belong to the simplest models in their kind, their combination results in a model that seems intractable mathematically and is very difficult to treat numerically – hence the rather limited system sizes used in the present study. It is surely of interest to find a different combination of Hamiltonian and SOC models that would exhibit a similar combination of thermodynamic and SOC criticality effects, yet would be easier to deal with.

Compared with the phase space of the standard Ising model, the phase space volume of the hybrid model is significantly reduced (from  $3^N$  down to  $a^N$  with  $a < 3$ ) in a non-local manner. Such reduction resembles that associated with lowering of the system dimensionality and hence may affect the critical properties of the system. We have shown that it actually decreases the number of possible phases. Even though our study indicates that the critical exponent  $\alpha$  in the hybrid model takes on the same value as in the Ising model, the question remains whether the two systems belong exactly to the same universality class and other exponents should be also examined. Another problem is to investigate the decay of correlation functions as  $T \downarrow T_c$ .

Last, but not least, our numerical results indicate that in the BTW model on a honeycomb lattice of linear size  $L \rightarrow \infty$ , the probabilities  $c_L^{(k)}$  to find  $k$  grains in



a given lattice site take on particularly simple values,  $c_{\infty}^{(0)} = 2/24$ ,  $c_{\infty}^{(1)} = 7/24$ , and  $c_{\infty}^{(2)} = 15/24$ . acknowledged.

### Acknowledgments

Support from Action de Recherche Concertée Program of the University of Liège (ARC 02/07-293) is gratefully

- 
- [1] H. J. Jensen, *Self-Organized Criticality* (Cambridge Univ. Press, Cambridge, 1998).
  - [2] R. Dickman, M. A. Muñoz, A. Vespignani, and S. Zapperi, *Braz. J. Phys.* **30**, 27 (2000).
  - [3] D. Sornette, A. Johansen, and I. Dornic, *J. Phys. I France* **5**, 325 (1995).
  - [4] A. Vespignani and S. Zapperi, *Phys. Rev. E* **57**, 6345 (1998).
  - [5] R. Meester and C. Quant, *Markov Proc. Rel. Fields* **11**, 355 (2005).
  - [6] P. Bak, C. Tang, and K. Wiesenfeld, *Phys. Rev. A* **38**, 364 (1988).
  - [7] D. Dhar, *Phys. Rev. Lett.* **64**, 1613 (1990).
  - [8] D. Dhar, *Physica A* **263**, 4 (1999).
  - [9] R. Meester, F. Redig, and D. Znamenski, *Markov Proc. Rel. Fields* **7**, 509 (2001).
  - [10] E. V. Ivashkevich and V. B. Priezzhev, *Physica A* **254**, 97 (1998).
  - [11] S. N. Majumdar and D. Dhar, *J. Phys. A: Math. Gen.* **24**, L357 (1991).
  - [12] E. V. Ivashkevich, *J. Phys. A: Math. Gen.* **27**, 3643 (1994).
  - [13] E. Dinaburg, C. Maes, S. Pirogov, F. Redig, and A. Rybko, *J. Stat. Phys.* **117**, 179 (2004).
  - [14] M. E. Fisher, *Rep. Prog. Phys.* **30**, 615 (1967).
  - [15] Y. Gefen, B. B. Mandelbrot, and A. Aharony, *Phys. Rev. Lett.* **45**, 855 (1980).
  - [16] J. Viana Lopes, Y. G. Pogorelov, J. M. Lopes Dos Santos, and R. Toral, *Phys. Rev. E* **70**, 026112 (2004).
  - [17] K. Binder and A. P. Young, *Rev. Mod. Phys.* **58**, 801 (1986).
  - [18] J. Jäckle, *Rep. Prog. Phys.* **49**, 171 (1986).
  - [19] S. N. Majumdar and D. S. Dean, *Phys. Rev. E* **66**, 056114 (2002).
  - [20] M. E. J. Newman and C. Moore, *Phys. Rev. E* **60**, 5068 (1999).
  - [21] D. Dhar and S. S. Manna, *Phys. Rev. E* **49**, 2684 (1994).
  - [22] N. Metropolis, A. W. Rosenbluth, M. N. Rosenbluth, A. H. Teller, and E. Teller, *J. Chem. Phys.* **21**, 1087 (1953).
  - [23] K. Binder, *Rep. Prog. Phys.* **60**, 487 (1997).
  - [24] P. Grassberger and S. S. Manna, *J. Phys. France* **51**, 1077 (1990).
  - [25] S. Lübeck and K. D. Usadel, *Phys. Rev. E* **55**, 4095 (1997).
  - [26] V. B. Priezzhev, *J. Stat. Phys.* **74**, 955 (1994).
  - [27] A. Rosengren and R. Häggkvist, *Phys. Rev. Lett.* **63**, 660 (1989).
  - [28] P. F. Fox and A. J. Guttmann, *J. Phys. C* **6**, 913 (1973).
  - [29] K. Vollmayr, J. D. Reger, M. Scheucher, and K. Binder, *Z. Phys. B* **91**, 113 (1993).
  - [30] R. Dickman, *Europhys. Lett.* **61**, 294 (2003).